ACS Sustainable Chemistry & Engineering

Research Article

pubs.acs.org/journal/ascecg

Green Chemistry of Zein Protein Toward the Synthesis of Bioconjugated Nanoparticles: Understanding Unfolding, Fusogenic Behavior, and Hemolysis

Aabroo Mahal,[§,∥] Poonam Khullar,*[,§] Harsh Kumar,[∥] Gurinder Kaur,[‡] Narpinder Singh,[⊥] Masoud Jelokhani-Niaraki,[†] and Mandeep Singh Bakshi*[,†]

[†]Department of Chemistry, Wilfrid Laurier University, Science Building, 75 University Ave. W., Waterloo, ON N2L 3C5, Canada

[‡]Nanotechnology Research Laboratory, College of North Atlantic, Labrador City, NL A2 V 2K7, Canada

[§]Department of Chemistry, B.B.K. D.A.V. College for Women, Amritsar 143005, Punjab, India

[∥]Department of Chemistry, Dr. B. R. Ambedkar National Institute of Technology, Jalandhar-144011, Punjab, India

[⊥]Department of Food Science and Technology, Guru Nanak Dev University, Amritsar 143005, Punjab, India

S *Supporting Information*

ABSTRACT: Green chemistry of industrially important zein protein was explored in aqueous phase toward the synthesis of bioconjugated gold (Au) nanoparticles (NPs), which allowed us to simultaneously understand the unfolding behavior of zein with respect to temperature and time. Synthesis of Au NPs was monitored with simultaneous measurements of UV−visible absorbance due to the surface plasmon resonance (SPR) of Au NPs that triggered the adsorption of zein on the NP surface and thus resulted in its unfolding. Surface adsorption of zein further controlled the crystal growth of Au NPs, which relied on the degree of unfolding and fusogenic behavior of zein due to its predominant hydrophobic nature. The latter property induced a marked blue shift in the SPR rarely observed in the growing NPs during the nucleation process. A greater unfolding of zein in fact was instrumental in generating zein-coated faceted NPs that were subjected to their hemolytic response for their possible use as drug release vehicles. Zein coating significantly reduced the hemolysis and made bioconjugated Au NPs the best models for biomedical applications in nanotechnology.

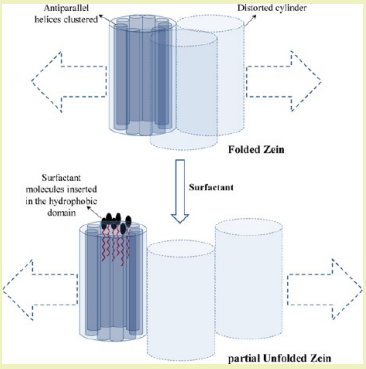

KEYWORDS: *Zein protein, Green chemistry, Unfolding, Bioconjugated nanoparticles, Hemolysis*

INTRODUCTION

Zein is an alcohol soluble corn storage protein with extensive industrial and food applications that is also widely used for coatings of paper cups, clothing fabrics, adhesives, and binders. It is clear, odorless, tasteless, edible, and hence used in processed foods and pharmaceuticals. It is deficient in essential amino acids (such as lysine and tryptophan) and hence is poor in nutritional quality. It contains high proportions of nonpolar amino acid residues (such as leucine, alanine, and proline), which render it water insoluble.[1,2] It is therefore one of the best bioingredients for moisture-resistant biodegradable protein films essential to replace environmental nonfriendly synthetic alternatives.[3−6] It possesses a highly robust structure that is made up of nine homologous repeat units arranged in an antiparallel distorted cylindrical form and stabilized by hydrogen bonds.[7−9] With all these versatile applications, little is known about its aqueous phase unfolding behavior and subsequent green chemistry. We believe a proper understanding about this will pave the way for its potential uses in aqueous phase as aqueous soluble biodegradable materials. Such materials can further find their applications in pharmaceuticals as drug delivery vehicles and UV-active contrast agents in biomedical diagnostics.

In order to understand the unfolding behavior of zein in aqueous phase, it has to be in the solubilized state. It can be made aqueous soluble in the presence of an appropriate surfactant that interacts simultaneously with its hydrophobic as well as hydrophilic domains.[10,11] Sodium dodecylsulfate (SDS) shows favorable interactions with zein and hence makes it aqueous soluble. Premicelle concentration of SDS makes zein−SDS a water-soluble complex by incorporating surfactant hydrocarbon chains in protein hydrophobic domains, while a much higher concentration drastically unfolds the protein and produces a highly water-soluble complex.[11] Similar interactions are reported with nonionic surfactants and lipids.[10] Fundamentally, it is much more complicated to understand the unfolding behavior of zein in comparison to other well-known water-soluble proteins such as bovine serum albumin (BSA) and cytochrome c (Cyc,c)[5,6,12] because zein possesses

Received: December 24, 2012
Revised: April 2, 2013
Published: April 12, 2013

predominant hydrophobic domains that make it water insoluble. Therefore, a proper understanding requires a systematic dismantling of its hydrophobic domains in aqueous phase under the effect of surfactant concentration and temperature. However, this is not the case with BSA and Cyc,c that become fully unfolded simply by increasing the temperature of aqueous phase to 70 °C[5,6] and also in the absence of any surfactant.[12] Thus, the best way to notice the unfolding[13] of zein in aqueous phase is to simultaneously use it as a reducing agent to generate Au NPs without the use of any additional stabilizing or reducing agent. A systematic unfolding exposes the reducing amino acids like cysteine to aqueous phase that simultaneously trigger the reduction reaction to convert Au(III) into Au(0) and produce Au NPs in the solution. In this way, both unfolding of zein as well as the synthesis of Au NPs are simultaneously happening in the aqueous phase and are complementary to each other due to the surface adsorption of zein on growing NPs. This helps us to understand the unfolding mechanism that can be precisely monitored by following the characteristic absorbance of Au NPs in the visible region due to their SPR. The higher the unfolding, the higher is the reduction potential of a protein to convert Au(III) into Au(0).[14] Unfolding is further related to the hydrophobicity and concentration of the surfactant.[15−17] Greater hydrophobicity and concentration unfolds zein to a greater extent, and that in turn is reflected by its stronger reduction potential in simultaneous synthesis of Au NPs. Thus, the nature of the surfactant is another important parameter that plays a crucial role in the unfolding behavior of zein.[18] A redominant hydrophobic surfactant is expected to induce greater unfolding in comparison to a less hydrophobic surfactant.

Because unfolded zein with its aqueous exposed hydrophobic domains is an amphipathic macromolecule, it is also expected to act as a stabilizing agent as well as a shape-directing agent for NPs.[19−21] Amphiphilic molecules prefer to adsorb at the interface where they can satisfy both their polar as well as nonpolar interactions. By doing so, they have the ability to completely block certain crystal planes and screen them completely from further participation in the crystal growth.[12] A complete blocking of a particular crystal plane is further related to the strength of an amphiphilic molecule. A stronger amphiphilic molecule can only completely passivate a particular crystal plane by forming a compact monolayer[22] that cannot be penetrated by freshly produced atoms to participate in crystal growth. Hence, crystal growth is directed to unpassivated crystal planes, and shape-controlled morphologies emerge. As the unfolded zein is involved in the simultaneous synthesis of Au NPs, the overall shape and structure of Au NPs synthesized are further related to the degree of unfolding. Completely unfolded protein is always a better shape-directing agent than partially unfolded protein[21] and hence produces ordered morphologies. Thus, the onset of the Au NPs formation and their shape and size are the best indicators of the zein unfolding behavior.

Our aim in this work is two fold: first, to understand the unfolding behavior of a highly hydrophobic water insoluble zein protein, and second, to understand its subsequent use in green chemistry as a shape-directing agent in the synthesis of protein−NP hybrid nanomaterials with several potential biomedical applications. We want to explore the possibilities that may allow zein-conjugated NPs for drug delivery vehicles in systemic circulation because zein is a proven well-known component of several food and pharmaceutical formulations, and hence, its bioconjugated NPs are also considered to be entirely nontoxic. For this purpose, we have employed such NPs to study their hemolytic response, which is believed to be the first step in exploring their biomedical applications in nanotechnology.

EXPERIMENTAL SECTION

Materials. Chloroauric acid ($HAuCl_4$), zein protein, sodium dodecylsulfate (SDS), sodium decylsulfate (SDeS), sodium tetradecylsulfate (STS), and sodium perfluorooctanoate (SPFO) were purchased from Aldrich. Double distilled water was used for all preparations.

Synthesis of Au NPs. First of all, zein was solubilized in an appropriate aqueous surfactant solution at room temperature. Then, aqueous mixtures (total of 10 mL) of zein (0.1−0.4%), surfactant (24 mM), and $HAuCl_4$ (0.25−1.0 mM) were taken in screw-capped glass bottles and kept in a water thermostat bath (Julabo F25) at precise 70 ± 0.1 °C for 6 h under static conditions. Zein acts as a weak reducing agent due to the presence of aqueous exposed reducing amino acids like cysteine and hence reduces Au(III) into Au(0) resulting in the color change from colorless to pink-purple.[6,12,13] The present surfactants are not expected to be involved in the reduction reaction in view of their complexation with zein protein.

$$Au^{3+}\,(aq) + \text{zein}\,(aq) + 3e^- \rightarrow Au^{o}\,(s) + \text{oxidizing products} \quad (1)$$

After 6 h, the samples were cooled to room temperature and kept overnight. They were purified from pure water at least three times to remove unreacted zein. Purification was done by collecting the Au NPs at 8000−10,000 rpm for 5 min after washing each time with distilled water.

Methods. All reactions were monitored simultaneously by UV−visible measurements (Shimadzu-Model No. 2450, double beam) in the wavelength range of 200−900 nm to observe the progress of the reactions by recording their absorbance due to the SPR. This instrument was equipped with a TCC 240A thermoelectrically temperature-controlled cell holder that allowed for measuring the spectrum at a constant temperature within ±1 °C.

Transmission electron microscopic (TEM) analysis was done on a JEOL 2010F at an operating voltage of 200 kV. The samples were prepared by mounting a drop of solution on a carbon-coated Cu grid and allowed to dry in the air. X-ray diffraction (XRD) patterns were recorded by using Bruker-AXS D8-GADDS with T_{sec} = 480. Samples were prepared by placing a concentrated drop of aqueous suspension on glass slides and then drying them in a vacuum desiccator. The polarity of the zein-coated NPs was determined by gel electrophoresis using TBE (tris-borate, 90 mM; ethylene diamine tetraacetic acid (EDTA), 2 mM, pH 8.0) buffer as a gel running medium. For this purpose, 1% of aqueous agarose solution was first heated to boiling with a microwave, poured into a gel plate, and allowed to harden. Then 20 μL of an aqueous NP solution was loaded in each gel well, and a direct voltage of 90 V was applied for 10 min to promote the movement of NPs. No staining agent was needed because the NP solutions in each case were colored (either pink or purple).

Hemolytic assay was performed to evaluate the response of zein-conjugated NPs on blood group B of red blood cells (RBCs) from a healthy human donor. Briefly, 5% suspension of RBCs was used for this purpose after three washings along with two concentrations (i.e., 50 and 100 μg/mL) of each NPs sample. A 1 mL packed cell volume (i.e., hematocrit) was suspended in 20 mL of 0.01 M phosphate-buffered saline (PBS). The positive control was RBCs in water, and it was prepared by spinning 4 mL of 5% RBCs suspension in PBS. PBS as supernatant was discarded, and pellet was resuspended in 4 mL of water. The negative control was PBS. All the readings were taken at 540 nm, i.e., absorption maxima of hemoglobin.

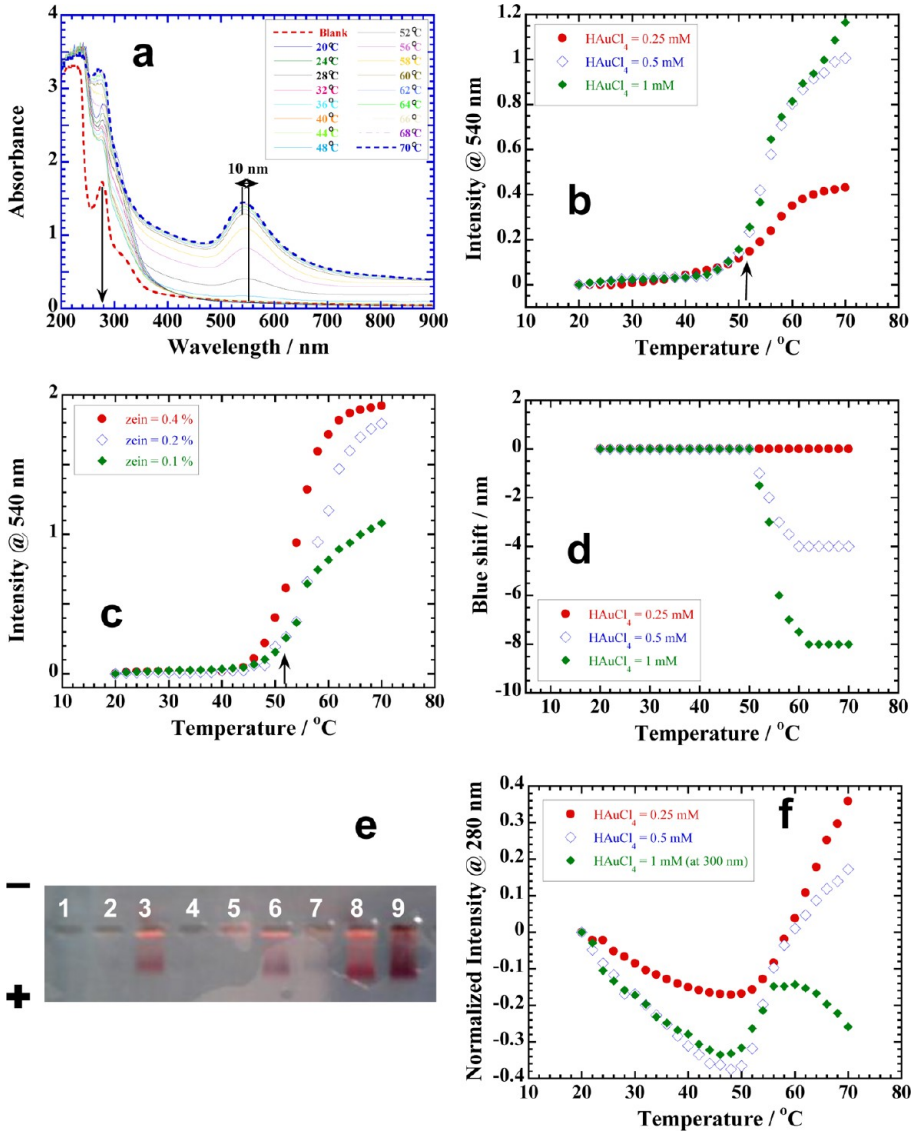

Figure 1. (a) UV−visible scans of a reaction with 0.1% zein (in aqueous 24 mM SDS) and 0.25 mM $HAuCl_4$ with temperature. (b) Plots of the variation of intensity at 540 nm with temperature for reactions with different amounts of $HAuCl_4$, and (c) for different amounts of zein. (d) Plots of blue shift in 540 nm peak for reactions with different amounts of $HAuCl_4$. (e) Gel electrophoresis of different samples (from 1 to 9) of zein conjugated NPs. Samples 1−3, 4−6, and 7−9 are made with 0.1, 0.2, and 0.4% zein, respectively. Samples 1, 2, and 3 are made, respectively, with 0.25, 0.5, and 1 mM $HAuCl_4$. The same is true for samples 4−6 and 7−9. (f) Plots of variation of intensity at 280 nm with temperature for reactions with different amounts of $HAuCl_4$. See details in the text.

RESULTS AND DISCUSSION

Unfolding and Synthesis of Au NPs. *Temperature Effect.* Unfolding of zein under the effect of temperature and its subsequent use in the synthesis of Au NPs depicts the reducing power of zein to convert Au(III) into Au(0). Once zein is solublilized in an aqueous surfactant solution, it can be used for the synthesis of Au NPs, which simultaneously helps us understand the unfolding behavior. Figure 1a depicts a typical reaction of 0.1% zein (in aqueous 24 mM SDS) and 0.25 mM $HAuCl_4$ with temperature. Aqueous zein gives a clear absorption around 280 nm mainly due to tyrosine (Tyr) and phenylalanine (Phe) nonpolar amino acid residues in comparison to tryptophan, which is present in a negligible amount. The intensity of this peak is dramatically affected as the growth of Au NPs proceeds from 20 to 70 °C, which is indicated by a prominent absorbance around 540 nm[5,6,13] due to the SPR. A variation in the intensity of the 540 nm peak with temperature for reactions with different concentrations of $HAuCl_4$ is shown in Figure 1b. A little increase in the intensity is observed up to 50 °C in all cases; thereafter, an exponential increase in the intensity indicates an instant growth in the nucleating centers. It shows that zein in aqueous SDS (24 mM) solution is not appreciably unfolded up to 50 °C, although the 24 mM concentration of SDS is about 3 times higher than its critical micelle concentration (8 mM, 25 °C)[23,24] and easily solubilizes 0.1% zein in aqueous phase but is unable to break the disulfide bonds. Solubilization of zein happens when hydrocarbon tails of SDS molecules are incorporated into the hydrophobic domains of zein while leaving anionic head groups in the aqueous phase.[11] This association provides an additional surface charge to the zein−SDS complex, thus making it water soluble. An increase in temperature further unfolds the secondary structure of zein first by breaking the hydrogen bonds operating among different cylindrical structures and then

dx.doi.org/10.1021/sc300176r | ACS Sustainable Chem. Eng. 2013, 1, 627−639

breaking the disulfide bonds to expose the cysteine residues in aqueous phase to initiate the reduction.[5,6] This happens around 50 °C in the presence of 24 mM SDS. Figure 1b shows minimum growth for 0.25 mM, while maximum growth is shown for 1 mM $HAuCl_4$. Almost all $AuCl_4^-$ ions of 0.25 mM $HAuCl_4$ are converted into the NPs up to 60 °C. After that their absorbance tends to be constant, while this is not the case for 0.5 and 1 mM $HAuCl_4$ even up to 70 °C, which is the maximum temperature we could accurately attain with our instrument to monitor the growth. This means that 0.1% zein generates enough reduction potential to completely reduce 0.25 mM Au(III) into Au(0) up to 60 °C but probably not sufficient to convert 0.5 and 1 mM Au(III) into nucleating centers.

Figure 1c shows the effect of zein concentration at a constant amount of 1 mM $HAuCl_4$. The 0.4% zein begins growth around 46 °C and almost completely converts all $AuCl_4^-$ ions into nucleating centers up to 60 °C. The 0.2% zein does it from 50 to 70 °C, while 0.1% zein never makes it to completion even up to 70 °C. A 4-fold rise in the concentration of zein (i.e., 4%) has practically little effect on initiating the reaction before 50 °C. It still initiates around 50 °C in all cases irrespective of the amount of zein used, which means that the unfolding clearly depends on the reaction temperature, while 24 mM SDS only helps in the solubilization of zein at room temperature, and actual unfolding of the secondary structure begins by breaking the hydrogen bonds around 50 °C. Thus, the 50 °C temperature is required to initiate the dismantling of the cylindrical structure of zein, which exposes the reducing amino acids to aqueous phase to start the reduction reaction.

Adsorption of Zein on Nanoparticle Surface. Unfolded zein in aqueous phase behaves like an amphiphile, which is best suited for its stabilizing as well as capping behaviors.[12] However, its predominant hydrophobic nature also makes it highly prone to fusogenic behavior[25,26] under the effect of temperature. This behavior is clearly visible in ∼10 nm blue shift in the absorbance of Au NPs (Figure 1a). During the nucleation process, usually several nucleating centers grow into individual NPs that exist in a colloidal state and produce single peak in the visible region (Figure 1a) due to their collective absorbance arising from SPR.[27] A red shift is observed if they aggregate in the solution,[28] but if the growing nucleating centers coalesce into a single NP, then a blue shift is observed.[29] We believe that the present blue shift of ∼10 nm is driven by the fusogenic behavior of capping zein (see the Time Effect section). Random collisions among the nucleating centers in aqueous phase facilitate the nonpolar interactions among the hydrophobic domains of capped zein. This promotes the interparticle fusion among the growing nucleating centers,[30] and hence, several small nucleating centers merge into a single NP resulting in a blue shift of ∼10 nm. A variation in the blue shift for reactions with different amounts of gold salt is depicted in Figure 1d. The blue shift starts as soon as nucleation starts around 50 °C and is maximum for 1 mM while insignificant for 0.25 mM $HAuCl_4$. Greater amounts of gold salt generate more nucleating centers, and hence, overall a greater magnitude of the blue shift in the absorbance of Au NPs is observed. This also indicates that the Au NPs thus produced are effectively capped by the surface adsorption of zein. This process further unfolds the protein, which has been previously reported for other proteins as well.[31−33] Gel electrophoresis (Figure 1e) authenticates the surface adsorption of zein, where zein capped NPs with a negative charge move toward the positive terminal of the battery. The negative charge is provided by the anionic head groups of SDS monomers embedded in the hydrophobic domains of zein through their hydrocarbon tails. Samples 1−3, 4−6, and 7−9 belong to 0.4, 0.2, and 0.1% zein with increasing amounts of gold salt (i.e., 0.25, 5, and 1 mM) in each case, respectively. Samples 7−9 show maximum displacement due to relatively less zein coating and hence less fusogenic effects in comparison to samples 1−3 that have maximum zein coatings and maximum fusogenic effects that induce maximum aggregation, which hindered the passage of zein-coated NPs through agrose gel. Likewise, samples 1, 4, and 7 show no displacement as they are maximumly affected due to the fusognic behavior because of their minimum number density caused by the minimum amount of gold salt (i.e., 0.25 mM) used in their synthesis.

The best way to monitor the surface adsorption of zein and its subsequent unfolding is to follow the change in intensity of absorption of nonpolar residues like Tyr and Phe around 280 nm. They are buried deep in the hydrophobic domains. Unfolding exposes them to aqueous phase and hence enhances their UV absorbance as more and more such residues are aqueously exposed. Surface adsorption of a protein is directly related to the overall shape and structure of its native state.[34] Globular proteins are considered to be less surface active than fibrous proteins. Surfactant-solubilized zein behaves more or less like a fibrous protein due to its amphiphilic nature that allows it to form a viscoelastic film on the NP surface. The film formation process further unfolds the protein and breaks the disulfide bridges to allow the formation of S−Au linkages. This process continues with the growth of the NP as a freshly produced surface attracts more protein that undergoes a further unfolding process. This is shown in Figure 1f where UV absorbance at 280 nm follows the growth process of NPs. It first shows a rapid decrease with a rise in temperature from 20−50 °C due to the dehydration of zein that strengthens the hydrophobic environment. Then, as soon as NPs start growing around 50 °C, likewise 280 nm absorbance increases and follows the growth process that clearly depicts a simultaneous surface adsorption and unfolding of zein. This is related to the number density of NPs produced in aqueous phase. A total of 0.25 mM $HAuCl_4$ produces a relatively minimum number of NPs, and hence, surface adsorption of zein continues from 50 to 70 °C (Figure 1f) although growth tends to limit around 60 °C (Figure 1b). This means that several layers of zein are deposited on the surface of NPs that keep unfolding and subsequently enhancing the intensity of the 280 nm peak. In fact, unfolded protein on the NP surface attracts the folded or partially unfolded free protein due to the seeding process,[35−37] which is quite common in protein−NP systems.[31,32] Both forms of protein (i.e., adsorbed and free) interact with each other to initiate self-aggregation. This is basically induced by the predominance of hydrophobic over hydrophilic interactions. Zein is predominantly a hydrophobic protein, and hence, nonpolar interactions promote fusogenic behavior among the hydrophobic domains of both forms of zein that facilitates its further deposition on a NP surface. On the contrary, when the number density of NPs is increased 4-fold (in the case of 1 mM $HAuCl_4$, Figure 1f), the intensity of the 280 nm peak abruptly decreases soon after 50 °C and the absorbance shifts from 280 to 300 nm though NPs continue to grow (Figure 1b). Now the same amount of zein is distributed over a 4-fold increased number of NPs, and nonpolar residues have relatively direct contact with the Au surface that causes the delocalization of an aromatic electron cloud and hence lowers

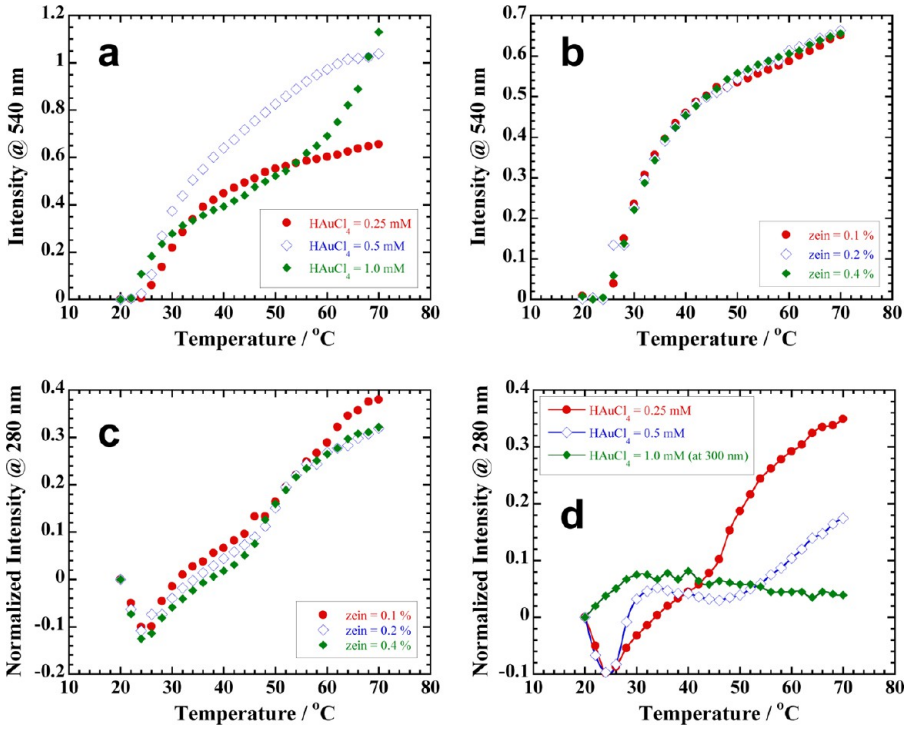

Figure 2. (a) Plots of the variation of intensity at 540 nm with temperature for reactions of 0.1% zein (in aqueous 24 mM SPFO) with different amounts of $HAuCl_4$ and (b) for different amounts of zein. (c) Plots of variation of intensity at 280 nm with temperature for reactions with different amounts of zein and (d) $HAuCl_4$. See details in the text.

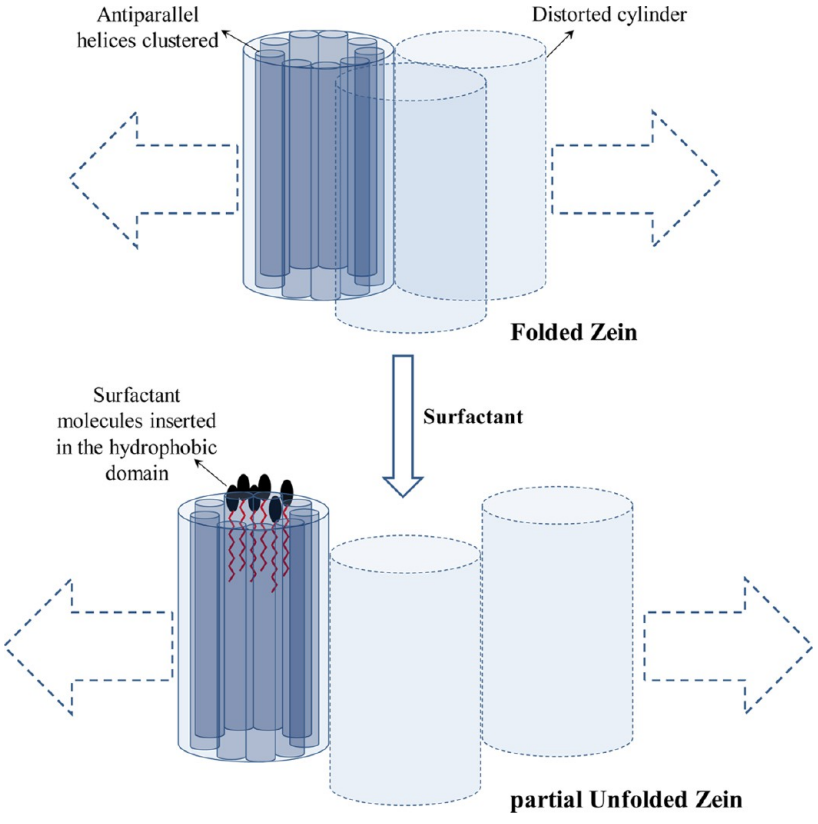

Figure 3. Schematic representation of the cylindrical structure of folded zein. Addition of surfactant induces unfolding by introducing its hydrocarbon tail into the predominantly hydrophobic cylinder. See details in the text.

the energy gap with the resulting absorbance shifted to a longer wavelength (300 nm). A 4-fold increase in the number density of the NPs is based on the fact that we obtained mostly hexagonal Au NPs of ~40 nm with no drastic change in the

dx.doi.org/10.1021/sc300176r | ACS Sustainable Chem. Eng. 2013, 1, 627−639

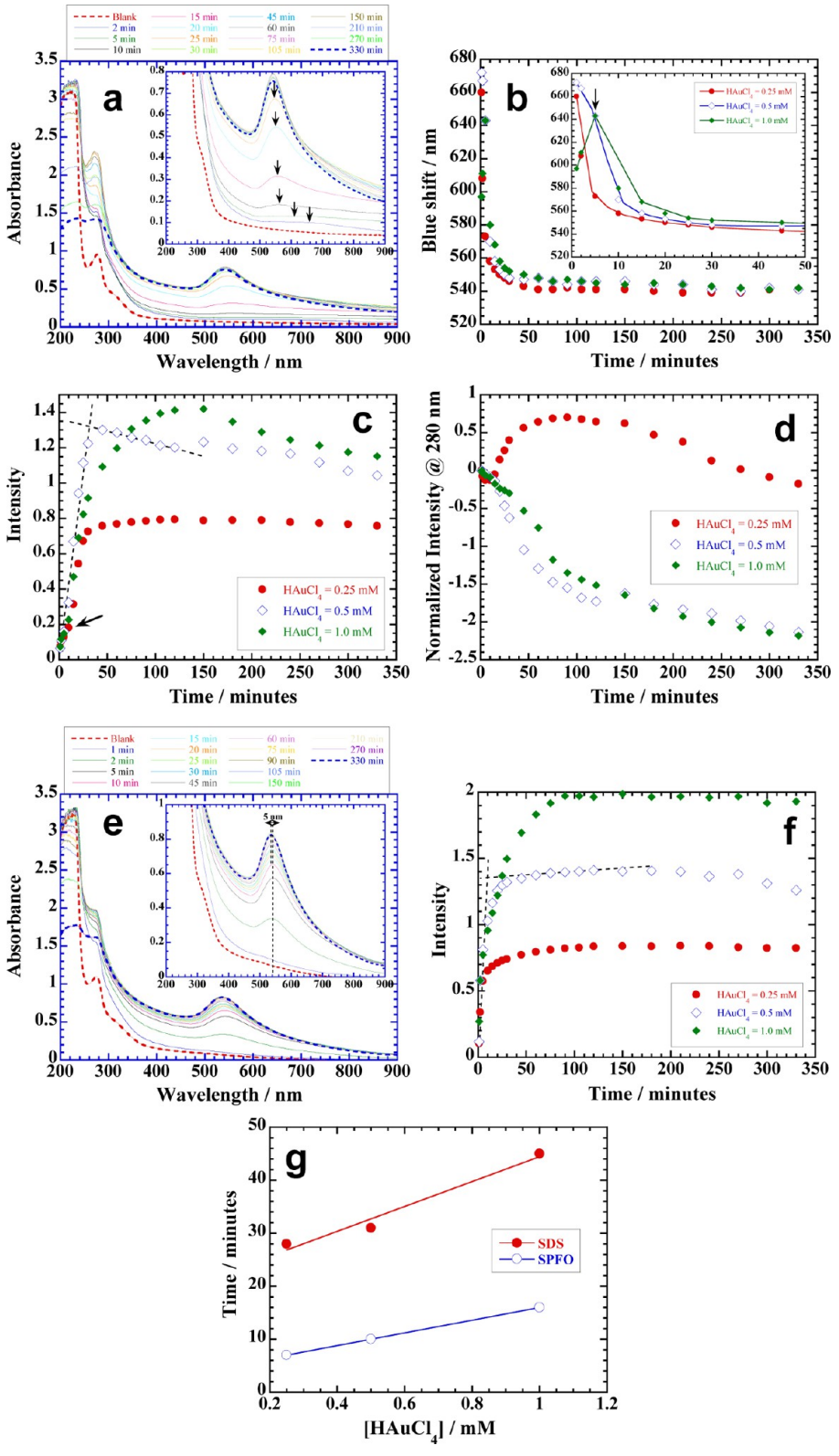

Figure 4. (a) UV−visible scans of a reaction with 0.1% zein (in aqueous 24 mM SDS) and 0.25 mM $HAuCl_4$ with time. Magnified view in inset shows a large blue shift with time indicated by black arrows. (b) Plots of the variation of the blue shift in 540 nm absorbance with time for reactions with different amounts of $HAuCl_4$. (c) Plots of the variation of intensity of Au NPs absorbance with time for reactions with different amounts of $HAuCl_4$. (d) Plots of variation of intensity at 280 nm with time for reactions with different amounts of $HAuCl_4$. (e) UV−visible scans of a reaction with 0.1% zein (in aqueous 24 mM SPFO) and 0.25 mM $HAuCl_4$ with time. (f) Variation in the intensity of Au NPs. See details in the text for reactions with different amounts of $HAuCl_4$. (g) Plots of maximum reaction time to complete reduction process vs the amount of $HAuCl_4$ for aqueous zein reactions in the presence of SDS and SPFO. See details in the text.

dx.doi.org/10.1021/sc300176r | *ACS Sustainable Chem. Eng.* 2013, 1, 627−639

shape and size within the amount of gold salt used, i.e., 0.25 − 1 mM. This is explained from TEM studies.

Effect of Surfactant Hydrophobicity. Because zein is predominantly a hydrophobic protein, the nature of the surfactant is expected to influence its solubility as well as unfolding. Replacing SDS (C12) with an equal amount of lower hydrophobicity SDeS (C10) does not induce any marked difference in the overall intensity variation profile of Au NPs absorbance (Figure S1, Supporting Information). Likewise, a similar variation is observed (Figure S2, Supporting Information) in the presence of STS (C14) with even higher hydrophobicity than SDS. Thus, a large variation in the hydrophobicity of a hydrocarbon chain from C10 to C14 practically induces little effect on the unfolding behavior of zein. On the contrary, if a hydrocarbon chain is replaced with a strongly hydrophobic fluorocarbon chain (Figure S3, Supporting Information), as in the case of SPFO, dramatic differences are observed.[38−40] First, nucleation begins around 25 °C (Figure 2a) rather than at 50 °C (Figure 1b), which is a huge drop in the nucleation temperature of Au NPs. This means that zein is now capable of converting Au(III) into Au(0) at 25 °C, which was not possible in the presence of a hydrocarbon surfactant (Figure 1b) even up to 50 °C and is only possible when a fluorocarbon chain unfolds zein to a much greater extent by dismantling the cylindrical hydrophobic domains and consequently exposing a greater number of cysteine residues to aqueous phase. Second, the reduction potential of unfolded zein is so strong that practically no difference in the growth kinetics of the nucleating centers is noticed within 0.1−0.4% of zein (Figure 2b) contrary to that in the presence of SDS (Figure 1c). In all cases, growth increases exponentially with equal magnitude starting from 25 °C with little difference in the profiles of reactions with different amounts of zein.

Similarly, surface adsorption and further unfolding of zein on growing the NP surface (Figure 2c) also begins along with the growth process as evident from the increasing intensity of nonpolar aromatic residues (Tyr and Phe). However, this variation becomes quite interesting with different amounts of gold salt as depicted in Figure 2d. Unfolding of zein follows the growth process of Figure 2a when 0.25 mM gold salt is used, but a 4-fold increase in the concentration (i.e., 1 mM gold salt) causes a slight decrease in the intensity around 30 °C, while NPs still continue to grow (Figure 2a). This situation arrives around 55 °C in the presence of SDS (Figure 1f) under identical conditions. Thus, both reduction (Figure 2a) and adsorption (Figure 2d) processes of unfolded zein shift to 30 °C in the presence of SPFO (from 55 °C in the presence of SDS) due to greater unfolding of the zein protein. Hence, unfolding of zein is entirely related to the hydrophobicity of a surfactant; a stronger hydrophobic surfactant like SPFO has the ability to dismantle the hydrophobic domains to a greater extent and also at a lower temperature. Each cylindrical hydrophobic domain of zein (Figure 3) is created by the antiparallel arrangement of nonpolar amino acid residues (mainly alanine, leucine, phenylalanine, valine, and proline).[7] Different hydrophobic domains are further associated with each other in a three-dimensional arrangement through hydrogen bonds that operate between the three pairs of polar amino acids (glutamine, asparagines, and sarine) located along the helical surface of each cylinder.[7] Insertion of the fluorocarbon tails into the hydrophobic domain (Figure 3) predominates the nonpolar interactions[38−40] between nonpolar amino acid residues and fluorocarbon tails over the hydrogen bonding that holds the three-dimensional arrangement and hence dismantles them into small aggregates of zein−SPFO complexes.[11] This happens to a much greater extent in the presence of SPFO rather than SDS and hence leads to greater unfolding.

Time Effect. *Zein + SDS Systems.* The above results help us understand the unfolding behavior of zein under the effect of temperature and hydrophobicity. This section explains the time effect at constant temperature of 70 °C. Figure 4a illustrates the time effect for a typical reaction of 0.1% zein (in the presence of 24 mM SDS) with 0.25 mM $HAuCl_4$, while the inset depicts the magnified view of the Au NPs absorbance with time that shows a significant blue shift of ∼170 nm (indicated by black arrows) over the reaction time. In the beginning of the reaction (within 2 min), a broad band appears around 680 nm, the intensity of which increases with time and becomes sharp and blue shifts to 540 nm. Its variation is shown in Figure 4b. Almost the same variation is observed for a reaction with 0.5 mM $HAuCl_4$, but 1 mM $HAuCl_4$ shows an initial red shift from 600 to 640 nm within 5 min of the reaction and then leads to the same blue shift (Figure 4b, inset). First of all, the blue shift refers to the same mechanism as discussed for Figure 1a, where a blue shift of just less than 10 nm occurred under the effect of temperature because zein was also undergoing a simultaneous unfolding mechanism with a rise in temperature. In contrast at a constant 70 °C, zein is already in its predominantly unfolded state and shows maximum capping ability through surface adsorption. Therefore, as soon as the nucleating centers are created, they are instantaneously capped by unfolded zein. The fusogenic behavior of zein induces aggregation among the capped NPs and causes a red shift within 5 min of the reaction for 1 mM $HAuCl_4$, but a relatively lower amount of 0.25 and 0.5 mM $HAuCl_4$ generate less numbers of aggregates with relatively insignificant red shifts (Figure 4b). However, the appearance of broad absorbance around 680 nm in the beginning of these reactions (within 2 min) suggests the presence of tiny NPs in aggregated states, otherwise it should have appeared around 520 nm[12,13] (the characteristic absorbance of colloidal Au NPs in an unassociated state). Thus, a blue shift of ∼170 nm again refers to a remarkable fusogenic behavior of unfolded zein that causes coalescence among the growing NPs and eventually leads to the formation of shape-controlled morphologies with characteristic absorbance around 540 nm (this is explained from microscopic studies). Similar results have been reported by Liz-Marzàn et al. for gold citrate.[27] The interparticle fusion is clearly evident from Figure 4c as well where the growth is depicted by an increase in the intensity and proceeds as long as the blue shift continues (Figure 4b); thereafter, it levels off or even slightly decreases because large NPs tend to settle. Likewise, the absorbance of nonpolar amino acid residues decreases (Figure 4d), especially in the case of reactions with 0.5 and 1 mM $HAuCl_4$. But the coalescence among much smaller amounts of NPs (0.25 mM $HAuCl_4$) seems to allow the deposition of zein that causes a slight increase in the intensity initially due to the unfolding.

Zein + SPFO Systems. UV−visible scans with time of a typical reaction of 0.1% zein (in the presence of 24 mM SPFO) with 0.25 mM $HAuCl_4$ are shown in Figure 4e. A magnified view of Au NPs absorbance with time (inset) depicts a slight blue shift of ∼5 nm as growth proceeds over the reaction time. Lack of fusogenic behavior due to dismantling of the hydrophobic domains causes an almost negligible blue shift in comparison to what is shown in Figure 4a. Growth profiles for

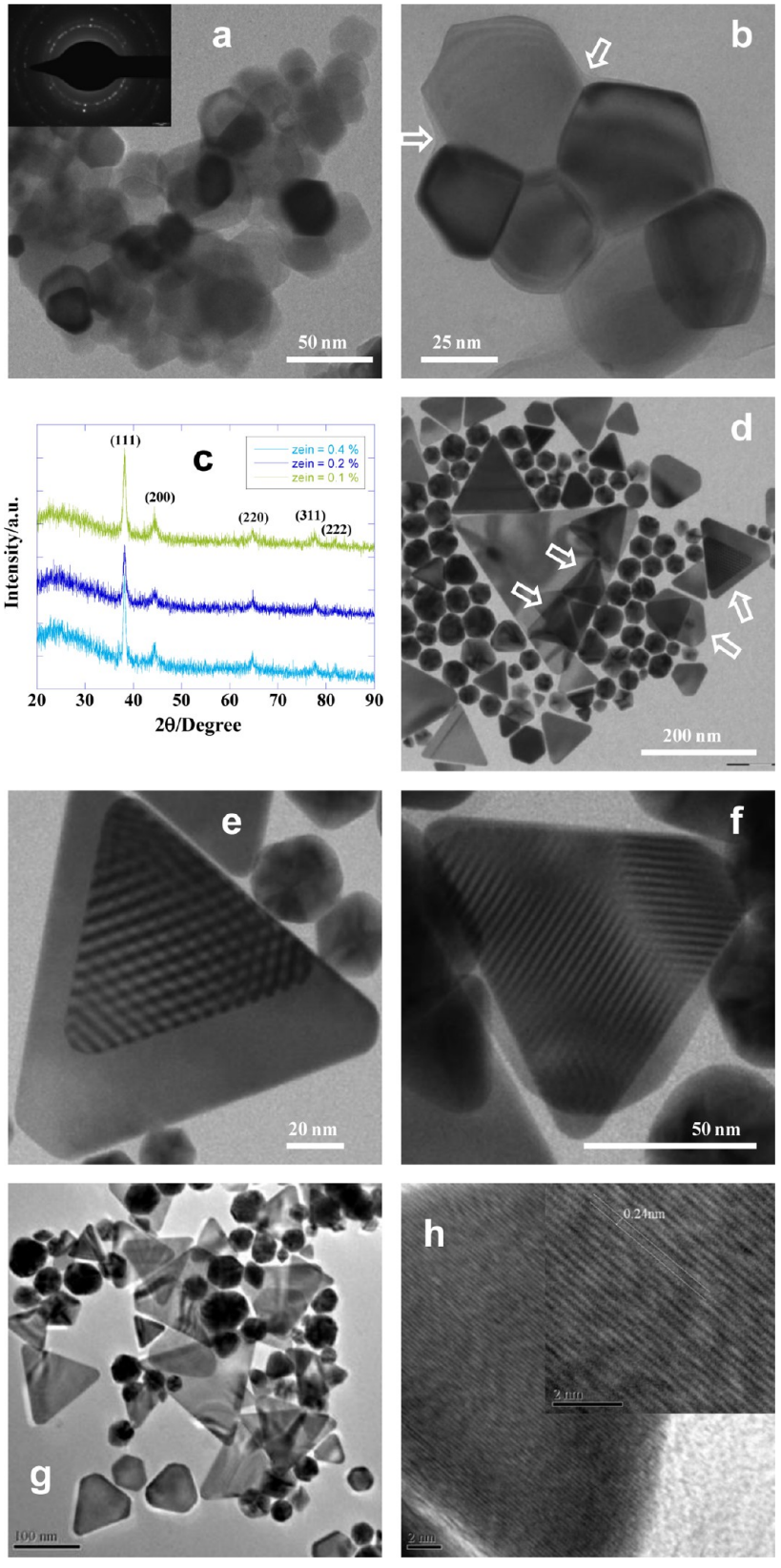

Figure 5. (a) TEM micrographs of small Au NPs prepared with a reaction of 0.1% zein (in aqueous 24 mM SDS) and 0.25 mM $HAuCl_4$. Note the highly aggregated NPs due to the fusogenic behavior of unfolded zein. (b) Close up view of faceted NPs in an aggregated state. (c) XRD patterns showing the fcc crystal structure with predominant growth on {111} crystal planes of Au NPs prepared with different amounts of zein. (d) TEM image showing several thin triangular nanoplates prepared with 0.5 mM $HAuCl_4$. (e) and (f) Close up view of two thin plates lying one above the other. (g) and (h) TEM micrographs of Au NPs and lattice fringes of a nanoplate, respectively, prepared with the same reaction but in aqueous 24 mM STS instead of SDS. See details in the text.

dx.doi.org/10.1021/sc300176r | *ACS Sustainable Chem. Eng.* 2013, 1, 627−639

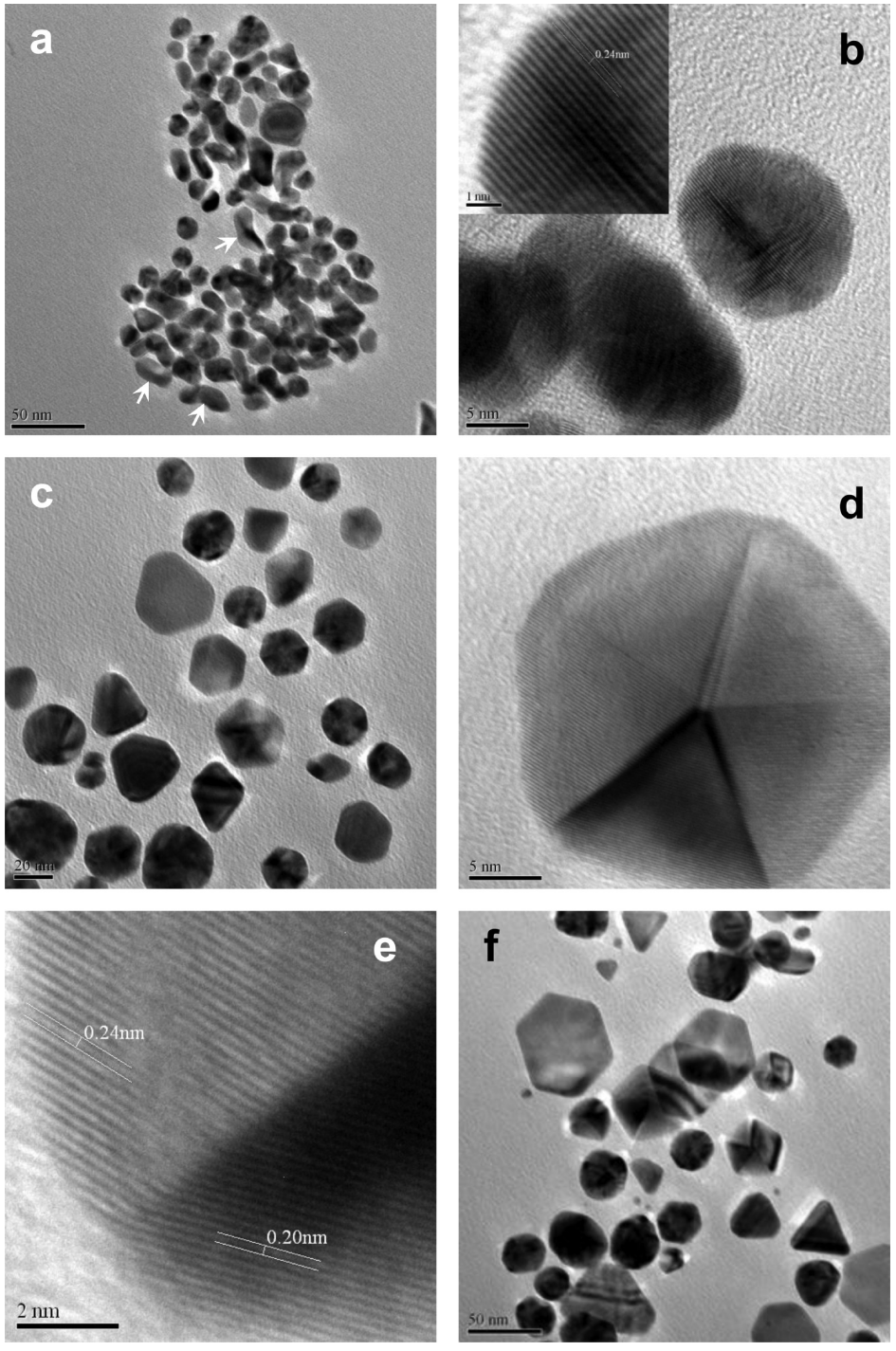

Figure 6. (a) TEM micrographs of small Au NPs prepared with a reaction of 0.1% zein (in aqueous 24 mM SPFO) and 0.25 mM $HAuCl_4$. Note the relatively unaggregated polyhedral NPs due to the weak fusogenic behavior of unfolded zein in the presence of SPFO. (b) Close up of a few NPs with lattice fringes. (c), (d), and (e) TEM images of well-defined NPs prepared with 0.5 mM $HAuCl_4$. (f) TEM image of NPs along with some nanoplates prepared with 1 mM $HAuCl_4$. See details in the text.

various reactions at different concentrations of gold salt (Figure 4f) are quite similar to that of Figure 4c, but growth reaches a limiting value in a much shorter period of time than in the presence of SDS. We determined the breaking points of each curve (as shown by dotted lines in Figure 4c and f) at a particular gold salt concentration where growth tends to be constant (plotted in Figure 4g). Two straight lines represent the maximum reaction time taken by the growth process at different gold salt concentrations in the presence of SDS and SPFO. One would notice that there is about a 4-fold increase in the reaction time when SDS is used instead of SPFO for the solubilization of zein. In other words, one can say that SPFO unfolds zein at least four times more than SDS.

Microscopic Studies. TEM images reveal the overall shape and aggregation behavior of Au NPs and demonstrate how effectively zein controls the shape through fusogenic behavior. Figure 5a show several small, thin, and crystalline (diffraction image in inset) NPs of about 30 ± 5 nm synthesized by a

dx.doi.org/10.1021/sc300176r | *ACS Sustainable Chem. Eng.* 2013, 1, 627−639

reaction of 0.1% zein (in the presence of 24 mM SDS) and 0.25 mM $HAuCl_4$ at 70 °C. A high degree of aggregation is observed among the NPs due to the fusogenic behavior of zein as depicted by UV−visible scans in Figure 4a and prevents its displacement in gel electrophoresis (Figure 1e, sample 1). Low contrast is basically due to the low diffraction from the highly thin NPs, while their overlapping and relatively thicker NPs produce dark contrast. Figure 5b provides clear evidence of this behavior where NPs with facets stick together through their flat surfaces (block arrows) due to the fusogenic behavior of zein. It should be mentioned that this effect is not because of any external factor like centrifugation and is induced only by the predominant hydrophobic nature of zein in the solution phase. XRD patterns are shown in Figure 5c, and all diffraction peaks can be indexed to Au fcc geometry with predominant growth at {111} crystal planes. When the amount of gold salt is increased from 0.25 to 1 mM, several large nanoplates are observed along with the smaller faceted mostly icosahedral NPs of 40 ± 8 nm (Figure 5d). Large nanoplates are considered to be the outcome of the smaller interparticles fusions[5] and are thus responsible for the prominent blue shift depicted in Figures 1d and 4b. The nanoplates are so thin that the smaller ones are lying either below or above the larger ones (block arrows in Figure 5d). These nanoplates are bound with {111} crystal planes that are completely coated with zein and are sticking together with other plates or plate-like NPs due to the fusogenic behavior of zein. A displacement of a 45° angle of the zone axis of the two nanoplates from each other highlights the hexagonal atomic arrangement of {111} crystal planes (Figure 5e), while a somewhat parallel arrangement reduces this effect (Figure 5f). Similarly, large nanoplates are predominantly produced in the presence of STS along with the mostly icosahedral particles (Figure 5g), and each nanoplate depicts the lattice spacing of 0.24 nm that originates from the {111} reflection of fcc gold (Figure 5h). We do not see any marked difference in the overall shape and size of the Au NPs produced in the presence of SDS or STS. This suggests a similar capping and stabilizing behavior of zein protein in the presence of both surfactants, and the higher hydrophobicity of STS does not induce any major change in the unfolding behavior of zein that would have a marked effect on the morphology of Au NPs. This observation is in line with similar UV−visible behavior of the growth kinetic of Au NPs by zein in the presence of both surfactants (Figure 1b and Figure S2, Supporting Information).

However, in the presence of SPFO, zein is much more unfolded (as explained from the UV−visible behavior, Figure 2) and is expected to have a much different capping and stabilizing behavior in comparison to that in the presence of SDS or STS. A reaction of 0.1% zein (in the presence of 24 mM SPFO) and 0.25 mM $HAuCl_4$ at 70 °C produces small polyhedral NPs of 25 ± 5 nm (Figure 6a) that are remarkably different from that of Figure 5a. First, they are not fused together as shown in Figure 5a,b, though some elongated particles (indicated by the white arrows) are the result of interparticle fusion. This is due to little fusogenic behavior of zein in the presence of SPFO as demonstrated by a relatively small blue shift of 5 nm (Figure 4e) in comparison to a large blue shift of 170 nm in the presence of SDS (Figure 4a). Second, NPs are polyhedral without facets contrary to what is shown in Figure 5b. They are single crystal and bound with {111} crystal planes as evident from the lattice fringes of 0.24 nm (Figure 6b). An increase in the concentration of gold salt to 0.5 mM however produces well-defined NPs, and most of them are dodecahedral with clear facets (Figure 6c,d) that are bound with both {111} and {200} crystal planes (Figure 6e). A further increase in the amount of gold salt to 1 mM also produces some nanoplates (Figure 6f), but the number density of dodecahedral is still much more. A relatively much weaker fusogenic behavior of zein in the presence of SPFO can be attributed to the dismantling of cylindrical hydrophobic domains to a much greater extent in comparison to that in the presence of SDS, thereby reducing their overall magnitude of hydrophobic interactions required for an effective fusogenic behavior. The hydrophobic interactions generated by the smaller hydrophobic domains are overwhelmed by the hydrophilic interactions generated by the predominant hydrophilic domains. This causes a significant decrease in the surface adsorption of zein as depicted in Figure 4d and hence consequently reducing the shape-directing effects. That is why the polyhedral morphologies of Figure 6b lack faceted NPs in comparison to that of Figure 5b, though they develop into faceted NPs (Figure 6d) later with an increase in concentration of gold salt. Apart from this, the lack of appropriate surface adsorption of zein allows the growing nuclei to grow into independent NPs without any kind of self-aggregation, and the growth is much rapid in comparison to that in the presence of SDS due to the greater extent of unfolding of zein by SPFO (Figure 4g). Thus, a rapid growth without an appropriate amount of stabilizing agent such as zein in this case induces anisotropic growth resulting in the formation of polyhedral morphologies in the first place.

Hemolysis. Although zein is a nontoxic protein and frequently used in the food industry, applications of zein-coated Au NPs as drug delivery vehicles require a proper understanding of their hemolytic behavior. NPs synthesized by using unfolded zein in the presence of SDS and SPFO were subjected to hemolytic response so as to understand the influence of degree of unfolding on the hemolysis. Because both surfactants form stable complexes with zein protein and no free surfactant is present in the solution after purification, hemolytic response is considered to be only due to the zein-coated NPs. Uncoated NPs that may be metal or nonmetal are highly toxic and show strong hemolysis.[41−43] Small mesoporous silica nanoparticles (~100 nm) adsorb to the surface of red blood cells (RBCs) without disturbing the membrane or morphology, while relatively larger ones induce a strong local membrane deformation leading to hemolysis.[44] Usually NP surface charge is the most important parameter in deciding the extent of hemolysis. Au NPs coated with cationic surfactant show a high degree of hemolysis.[13] Likewise, fullerenes bearing different numbers of cationic surface moieties show hemolytic tendency that is proportional to the number of attached cationic surface groups. The presence of unprotected primary amines (positive charges) on the surface of polyamidoamine (PAMAM),[45] carbosilane,[46] polypropylene imine (PPI),[47−49] and polylysine (PLL)[50] dendrimers are also associated with erythrocyte damage.

The hemolysis of the present samples is directly related to the extent of zein coating (Figure 7a) and does not show any mark dependence within the range of the shape and size of the present NPs. Samples 1−3 are made with 0.2% zein, while samples 4−6 are made with 0.1% zein, with increasing amounts of gold salt (0.25, 0.5, and 1 mM, respectively) in the presence of SDS. Samples 4−6 with almost half the amount of zein coating show more than a 3-fold higher hemolytic response than samples 1−3. On the other hand, samples 7−9 are made with 0.1% zein in the presence of SPFO, which show little

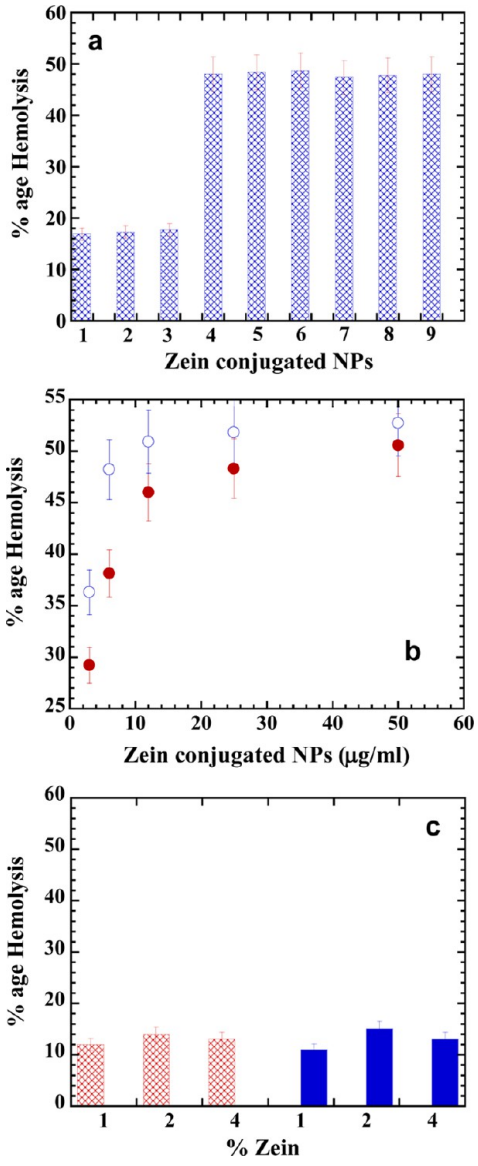

Figure 7. (a) Percentage of hemolysis for various zein-coated NPs samples. Samples 1−3 made with 0.2% zein in the presence of SDS with 0.25, 0.5, and 1 mM $HAuCl_4$. Likewise samples 4−6 and 7−9 are made with 0.1% zein in the presence of SDS and SPFO, respectively. (b) Variation of percentage hemolysis with the amount of NPs prepared with 0.1% zein in the presence of SDS (filled circles) and SPFO (empty circles). (c) Control experiments showing the percentage hemolysis by zein−SDS and zein−SPFO complexes in the absence of NPs. SDS = SPFO = 24 mM; zein = 0.1, 0.2, and 0.4%. See details in the text.

difference in their hemolytic response from that of samples 4−6 made in the presence of SDS. This is quite strange because we observed a marked difference in the magnitude of unfolding of zein in the presence of SDS and SPFO from UV−visible and TEM analysis. It demonstrates that probably the zein coating is more important in deciding the degree of hemolysis rather than the degree of unfolding because zein is basically predominantly a hydrophobic protein. Figure 7b supports this where a variation in the dose of NPs with the percentage hemolysis is presented for samples 4 and 7 (made with 0.1% zein in the presence of SDS and SPFO, respectively) of Figure 7a. In both cases, hemolysis increases instantaneously with an increase in the amount of NPs before tending to a constant value because the insufficient amount of coating (0.1% zein) induces an instant hemolysis and depends on the number density of NPs. Apart from this, another set of control experiments in the absence of NPs and presence of zein (Figure 7c) for water-soluble zein+SDS and zein+SPFO complexes show no marked dependence of hemolysis on the mount of zein. In other words, the hemolysis is not that significant when zein exists in the aqueous solubilized state rather when it is adsorbed on the NP surface, which means that hemolysis is primarily carried out by the NP surface interactions with the cell membrane and its deformation as reported by other authors.[41−44]

UV−visible studies in Figures 1f and 2d clearly demonstrate the NP surface adsorption of zein that consequently further unfolds its secondary structure and hence exposes its hydrophobic domains. These nonpolar domains in fact screen the electrostatic interactions operating between the hydrophilic domains of unfolded zein or an uncoated NP surface and that of the red blood cell membrane proteins. The NPs coated with 0.2% zein show significantly lower hemolysis because of an effective passivation of electrostatic interactions in comparison to that of 0.1% zein. The red blood cell membrane consists of three layers with glycocalyx on the exterior, protein network on the anterior, and lipid bilayer in between the two. The glycoprotein[51] and lipid bilayer[52] are highly susceptible to hydrophobic interactions and thus are responsible for the rupturing of the cell membranes. In this way, hemolysis can be avoided if properly coated NPs with zein can be used for drug release vehicles in the systemic circulation for biomedical applications.

CONCLUDING REMARKS

The results conclude that industrially important nontoxic zein protein can very well be used in the green synthesis of bioconjugated nanoparticles so as to expand its applications in nanotechnology and especially in the biomedical fields. We observed that the green synthesis simultaneously helps in evaluating the physiochemical behavior of zein such as unfolding and fusogenic properties in the aqueous phase. Both properties closely control the growth process of Au NPs and thus help in the formation of shape-controlled morphologies. Because of the amphiphilic nature of unfolded zein, it readily adsorbs on the NP surface and thus generates bioconjugated NPs suitable for drug release vehicles in the systemic circulation. Zein coating dramatically reduces the toxic and hemolytic effects of Au NPs and thus makes them suitable models for appropriate biomedical applications.

ASSOCIATED CONTENT

Supporting Information

UV−visible spectra. This material is available free of charge via the Internet at http://pubs.acs.org.

AUTHOR INFORMATION

Corresponding Author

*E-mail: ms_bakshi@yahoo.com (M.S.B.), virgo16sep2005@gmail.com (P.K.).

Notes

The authors declare no competing financial interest.

ACKNOWLEDGMENTS

These studies were partially supported by financial assistance under Article 27.8 of the CAS agreement of WLU, Waterloo.

Dr. Gurinder Kaur thankfully acknowledges the financial support provided by the Research and Development Council (RDC) of Newfoundland and Labrador, NSERC, and the Office of Applied Research at CNA. Research grants from DST (ref #SERB/F/0328/2012-13) and CSIR (ref #01(2683)/12), New Delhi, India, are also thankfully acknowledged.

REFERENCES

(1) Wu, S. W.; Myers, D. J.; Johnson, L. A. Factors affecting yield and composition of zein extracted from commercial corn gluten meal. *Cereal Chem.* **1997b**, *74*, 258−263.

(2) Pomes, A. F. Zein. In *Encyclopedia of Polymer Science and Technology: Plastics, Resins, Rubbers, Fibers*; Mark, H. F.; Gaylord, N. G.; Bikales, N. M., Eds.; New York: Interscience Publishers, 1971; Vol. 15, pp 125−132.

(3) Alkan, D.; Aydemir, L. Y.; Arcan, I.; Yavuzdurmaz, H.; Atabay, H. I.; Ceylan, C.; Yemenicioglu, A. Development of flexible antimicrobial packaging materials against *Campylobacter jejuni* by incorporation of gallic acid into zein-based films. *J. Agric. Food Chem.* **2011**, *59*, 11003−11010.

(4) Romero-Bastida, C. A.; Flores-Huicochea, E.; Martin-Polo, M. O.; Velazquez, G.; Torres, J. A. Compositional and moisture content effects on the biodegradability of zein/ethylcellulose film. *J. Agric. Food Chem.* **2004**, *52*, 2230−2235.

(5) Bakshi, M. S.; Kaur, H.; Khullar, P.; Banipal, T. S.; Kaur, G.; Singh, N. Protein films of bovine serum albumen conjugated gold nanoparticles: A synthetic route from bioconjugated nanoparticles to biodegradable protein films. *J. Phys. Chem. C* **2011**, *115*, 2982−2992.

(6) Bakshi, M. S.; Kaur, H.; Banipal, T. S.; Singh, N.; Kaur, G. Biomineralization of gold nanoparticles by lysozyme and cytochrome c and their applications in protein film formation. *Langmuir* **2010**, *26*, 13535−13544.

(7) Argos, P.; Pedersen, K.; Marks, M. D.; Larkins, B. A. A structural model for maize zein proteins. *J. Biol. Chem.* **1982**, *257*, 9984−9990.

(8) Shukla, R.; Cheryan, M. Zein: The industrial protein from corn. *Ind. Crops Prod.* **2001**, *13*, 171−192.

(9) Momany, F. A.; Sessa, D. J.; Lawton, J. W.; Selling, G. W.; Hamaker, S. A. H.; Willett, J. Structural Characterization of α-Zein. *J. Agric. Food Chem.* **2005**, *54*, 543−547.

(10) Moore, P. N.; Puvvada, S.; Blankschtein, D. Role of the surfactant polar head structure in protein−surfactant complexation: Zein protein solubilization by SDS and by SDS/$C_{12}E_n$ surfactant solutions. *Langmuir* **2003**, *19*, 1009−1016.

(11) Deo, N.; Jockusch, S.; Turro, N. J.; Somasundaran, P. Surfactant interactions with zein protein. *Langmuir* **2003**, *19*, 5083−5088.

(12) Bakshi, M. S. Nanoshape control tendency of phospholipids and proteins: Protein−nanoparticle composites, seeding, self-aggregation, and their applications in bionanotechnology and nanotoxicology. *J. Phys. Chem. C* **2011**, *115*, 13947−13960.

(13) Khullar, P.; Singh, V.; Mahal, A.; Dave, P. N.; Thakur, S.; Kaur, G.; Singh, J.; Singh Kamboj, S.; Singh Bakshi, M. Bovine serum albumin bioconjugated gold nanoparticles: Synthesis, hemolysis and cytotoxicity towards cancer cell lines. *J. Phys. Chem. C* **2012**, *116*, 8834−8843.

(14) Ibrahimkutty, S.; Kim, J.; Cammarata, M.; Ewald, F.; Choi, J.; Ihee, H.; Plech, A. Ultrafast Structural dynamics of the photo-cleavage of protein hybrid nanoparticles. *ACS Nano* **2011**, *5*, 3788−3794.

(15) Gunning, P. A.; Mackie, A. R.; Gunning, A. P.; Woodward, N. C.; Wilde, P. J.; Morris, V. J. The effect of surfactant type on surfactant−protein interactions at the air−water interface. *Biomacromolecules* **2004**, *5*, 984−991.

(16) Stenstam, A.; Topgaard, D.; Wennerstrom, H. Aggregation in a protein−surfactant system. The interplay between hydrophobic and electrostatic interactions. *J. Phys. Chem. B* **2003**, *107*, 7987−7992.

(17) Semenova, M. G.; Belyakova, L. E.; Polikarpov, Y. N.; Il'in, M. M.; Istarova, T. A.; Anokhina, M. S.; Tsapkina, E. N. Thermodynamic analysis of the impact of the surfactant−protein interactions on the molecular parameters and surface behavior of food proteins. *Biomacromolecules* **2006**, *1*, 101−113.

(18) Chakraborty, T.; Chakraborty, I.; Moulik, S. P.; Ghosh, S. Physicochemical and conformational studies on BSA−surfactant interaction in aqueous medium. *Langmuir* **2009**, *25*, 3062−3074.

(19) Bakshi, M. S.; Jaswal, V. S.; Kaur, G.; Simpson, T. W.; Banipal, P. K.; Banipal, T. S.; Possmayer, F.; Petersen, N. O. Biomineralization of BSA-chalcogenide Bioconjugate nano- and micro-crystals. *J. Phys. Chem. C* **2009**, *113*, 9121−9127.

(20) Kaur, G.; Iqbal, M.; Bakshi, M. S. Biomineralization of fine selenium crystalline rods and amorphous spheres. *J. Phys. Chem. C* **2009**, *113*, 13670−13676.

(21) Bakshi, M. S.; Thakur, P.; Kaur, G.; Kaur, H.; Banipal, T. S.; Possmayer, F.; Petersen, N. O. Stabilization of PbS nanocrystals by bovine serum albumin in its native and denatured states. *Adv. Funct. Mater.* **2009**, *19*, 1451−1458.

(22) Bakshi, M. S.; Possmayer, F.; Petersen, N. O. Role of different phospholipids in the synthesis of pearl-necklace type gold−silver bimetallic nanoparticles as bioconjugate materials. *J. Phys. Chem. C* **2007**, *111*, 14113−14124.

(23) Bakshi, M. S. Micelle formation by sodium dodecyl sulfate in water additive systems. *Bull. Chem. Soc. Jpn.* **1996**, *69*, 2723−2729.

(24) Bakshi, M. S. Micelle formation by anionic and cationic surfactants in binary aqueous solvents. *J Chem. Soc., Faraday Trans.* **1993**, *89*, 4323−4326.

(25) Csiszar, A.; Hersch, N.; Dieluweit, S.; Biehl, R.; Merkel, R.; Hoffmann, B. Novel fusogenic liposomes for fluorescent cell labeling and membrane modification. *Bioconjugate Chem.* **2010**, *21*, 537−543.

(26) El Kirat, K.; Lins, L.; Brasseur, R.; Dufrene, Y. F. Fusogenic titled peptides induce nanoscales holes in supported in phosphatidylcholine bilayers. *Langmuir* **2005**, *21*, 3116−3121.

(27) Rodríguez-González, B.; Mulvaney, P.; Liz-Marzán, L. M. An electrochemical model for gold colloid formation via citrate reduction. *Z. Phys. Chem.* **2007**, *221*, 415−426.

(28) Chandrasekharan, N.; Kamat, P. V. Assembling gold nanoparticles as nanostructured films using an electrophoretic approach. *Nano Lett.* **2001**, *1*, 67−70.

(29) Ganguli, M.; Babu, J. V.; Maiti, S. Complex formation between cationically modified gold nanoparticles and DNA: An atomic force microscopic study. *Langmuir* **2004**, *20*, 5165−5170.

(30) Botsaris, G. D.; Denk, E. G.; Ersan, G. S.; Kirwan, D. J.; Margolis, G.; Ohara, M.; Reid, R. C.; Tester, J. *Industrial & Engineering Chemistry* **1969**, *61*, 86−113.

(31) Zhang, D.; Neumann, O.; Wang, H.; Yuwono, V. M.; Barhoumi, A.; Perham, M.; Hartgerink, J. D.; Wittung-Stafshede, P.; Halas, N. J. Gold nanoparticles can induce the formation of protein-based aggregates at physiological pH. *Nano Lett.* **2009**, *9*, 666−671.

(32) Slocik, J. M.; Tam, F.; Halas, N. J.; Naik, R. R. Peptide-assembled optically responsive nanoparticle complexes. *Nano Lett.* **2007**, *7*, 1054−1058.

(33) Neumann, O.; Zhang, D.; Tam, F.; Lal, S.; Wittung-Stafshede, P.; Halas, N. J. Direct optical detection of aptamer conformational changes induced by target molecules. *Anal. Chem.* **2009**, *81*, 10002−10006.

(34) Paquin, P.; Britten, M.; Laliberté, M.-F.; Boulet, M. Interfacial Properties of Milk Casein Proteins. In *Proteins at Interfaces*; Brash, J. L., Horbett, T. A., Eds.; ACS Symposium Series 343; American Chemical Society: Washington, DC, 1987; Chapter 42, pp 677−686.

(35) Shukla, U. J.; Marino, H.; Huang, P. S.; Mayo, S. L.; Love, J. J. A designed protein interface that blocks fibril formation. *J. Am. Chem. Soc.* **2004**, *126*, 13914−13915.

(36) Yamaguchi, K-i.; Matsumoto, T.; Kuwata, K. Critical region for amyloid fibril formation of mouse prion protein: unusual amyloidgenic properties of the helix 2 peptide. *Biochemistry* **2008**, *47*, 13242−13251.

(37) Dzwolak, W.; Loksztejn, A.; Galinska-Rakoczy, A.; Adachi, R.; Goto, Y.; Rupnicki, L. Conformational indeterminism in protein misfolding: Chiral amplification on amyloidogenic pathway of insulin. *J. Am. Chem. Soc.* **2007**, *129*, 7517−7522.

(38) Barthelemy, P.; Tomao, V.; Selb, J.; Chaudier, Y.; Pucci, B. Fluorocarbon−hydrocarbon non-ionic surfactant mixtures: A study of their miscibility. *Langmuir* **2002**, *18*, 2557−2563.
(39) Asakawa, T.; Hisamatsu, H.; Miyagishi, S. Experimental verification of demixing micelles composed of fluorocarbon and hydrocarbon surfactants via fluorescence-quenching method. *Langmuir* **1996**, *12*, 1204−1207.
(40) Mukerjee, P.; Handa, T. Adsorption of fluorocarbon and hydrocarbon surfactants to air−water, hexane−water, and perfluorohexane−water interfaces: Relative affinities and fluorocarbon−hydrocarbon nonideality effects. *J. Phys. Chem.* **1981**, *85*, 2298−2303.
(41) Lin, Y. S.; Haynes, C. L. Impacts of mesoporous silica nanoparticle size, pore ordering, and pore integrity on hemolytic activity. *J. Am. Chem. Soc.* **2010**, *132*, 4834−4842.
(42) Lin, Y. S.; Haynes, C. L. Synthesis and characterization of biocompatible and size-tunable multifunctional porous silica nanoparticles. *Chem. Mater.* **2009**, *21*, 3979−3986.
(43) Dobrovolskaia, M. A.; Clogston, J. D.; Neun, B. W.; Hall, J. B.; Patri, A. K.; McNeil, S. E. Method for analysis of nanoparticle hemolytic properties in vitro. *Nano Lett.* **2008**, *8*, 2180−2187.
(44) Zhao, Y.; Sun, X.; Zhang, G.; Trewyn, B. G.; Slowing, I. I.; Lin, V. S. Y. Interaction of mesoporous silica nanoparticles with human red blood cell membranes: Size and surface effects. *ACS Nano* **2011**, *5*, 1366−1375.
(45) Domanski, D. M.; Klajnert, B.; Bryszewska, M. Influence of PAMAM dendrimers on human red blood cells. *Bioelectrochemistry* **2004**, *63*, 189−191.
(46) Bermejo, J. F.; Ortega, P.; Chonco, L.; Eritja, R.; Samaniego, R .; Mullner, M.; de Jesus, E.; de la Mata, F. J.; Flores, J. C.; Gomez, R.; Munoz-Fernandez, A. Water-soluble carbosilane dendrimers: Synthesis biocompatibility and complexation with oligonucleotides; evaluation for medical applications. *Chem.—Eur. J.* **2007**, *13*, 483−495.
(47) Agashe, H. B.; Dutta, T.; Garg, M.; Jain, N. K. Investigations on the toxicological profile of functionalized fifth-generation poly (propylene imine) dendrimer. *J. Pharm. Pharmacol* **2006**, *58*, 1491−1498.
(48) Dutta, T.; Agashe, H. B.; Garg, M.; Balakrishnan, P.; Kabra, M.; Jain, N. K. Poly (propyleneimine) dendrimer based nanocontainers for targeting of efavirenz to human monocytes/macrophages in vitro. *J. Drug Targeting* **2007**, *15*, 89−98.
(49) Malik, N.; Wiwattanapatapee, R.; Klopsch, R.; Lorenz, K.; Frey, H.; Weener, J. W.; Meijer, E. W.; Paulus, W.; Duncan, R. Dendrimers: Relationship between structure and biocompatibility in vitro, and preliminary studies on the biodistribution of ^{125}I-labelled polyamidoamine dendrimers in vivo. *J. Controlled Release* **2000**, *65*, 133−148.
(50) Shah, D. S.; Sakthivel, T.; Toth, I.; Florence, A. T.; Wilderspin, A. F. DNA transfection and transfected cell viability using amphipathic asymmetric dendrimers. *Int. J. Pharm.* **2000**, *208*, 41−48.
(51) Derjaguin, B.; Landau, L. Theory of the stability of strongly charged lyophobic sols and of the adhesion of strongly charged particles in solution of electrolytes. *Acta Phys. Chem. URSS* **1941**, *14*, 633−662.
(52) Dedinaite, A.; Lundin, M.; Macakova, L.; Auletta, T. Mucin−chitosan complexes at the solid−liquid interface: Multilayer formation and stability in surfactant solutions. *Langmuir* **2005**, *21*, 9502−9509.